

## Composite materials based on nanoporous SiO<sub>2</sub>-matrices and TiO<sub>2</sub> nanoparticles

*O.N.Bezkrounaya*<sup>1</sup>, *I.M.Pritula*<sup>1</sup>, *O.M.Vovk*<sup>1</sup>, *Yu.A.Gurkalenko*<sup>2</sup>,  
*A.N.Shaposhnik*<sup>3</sup>, *D.S.Sofronov*<sup>3</sup>, *Y.V.Taranets*<sup>1</sup>

<sup>1</sup>Institute for Single Crystals, STC "Institute for Single Crystals",  
National Academy of Sciences of Ukraine,  
60 Nauky Ave., 61001 Kharkiv, Ukraine

<sup>2</sup>Institute for Scintillation Materials, SSI "Institute for Single Crystals",  
National Academy of Sciences of Ukraine, 60 Nauky Ave.,  
61001 Kharkiv, Ukraine

<sup>3</sup>Division of Functional Materials Chemistry, STC "Institute for Single Crystals", National Academy of Sciences of Ukraine, 60 Nauky Ave.,  
61001 Kharkiv, Ukraine

*Received July 12, 2020*

SiO<sub>2</sub>:TiO<sub>2</sub> composites were obtained by saturation of SiO<sub>2</sub>-matrices (with a porosity of ~ 30 % and ~ 42 %) with a suspension of TiO<sub>2</sub> nanoparticles and subsequent annealing to 700°C. It was shown that, due to annealing of the composites in the temperature range of 400–700°C, there was observed agglomeration of TiO<sub>2</sub> nanoparticles in the pores of the SiO<sub>2</sub>-matrices, that manifested itself in an increase of the absorption in wavelength range of 390–800 nm. The presence of diffraction rings in the electron microdiffraction images confirms formation of TiO<sub>2</sub> crystallites in SiO<sub>2</sub>:TiO<sub>2</sub> composites. The content of titanium in the composite less than 1 % relative to silicon did not allow to reveal crystalline TiO<sub>2</sub> phase in the composites by powder X-ray diffraction method. TiO<sub>2</sub> is probably present in the composites based on SiO<sub>2</sub>-matrices with high porosity both in the form of crystallites and in amorphous state.

**Keywords:** SiO<sub>2</sub>-matrices, TiO<sub>2</sub> nanoparticles, composites, absorption.

**Композитні матеріали на основі нанопористих SiO<sub>2</sub>-матриць і наночастинок TiO<sub>2</sub>.**  
*О.М.Безкровна, І.М.Притула, О.М.Вовк, Ю.О.Гуркаленко, А.М.Шапошнік, Д.С.Софронов, Ю.В.Таранець*

Отримано композити SiO<sub>2</sub>:TiO<sub>2</sub> шляхом насичення SiO<sub>2</sub>-матриць (з пористістю ~ 30 % і ~ 42 %) суспензією наночастинок TiO<sub>2</sub> і подальшим відпалом до температури 700°C. Показано, що у результаті відпалу композитів в інтервалі температур 400–700°C спостерігається агломерація наночастинок TiO<sub>2</sub> у порах SiO<sub>2</sub>-матриці, що проявляється в збільшенні поглинання в інтервалі довжин хвиль 390–800 нм. Утворення кристалітів TiO<sub>2</sub> у композитах SiO<sub>2</sub>:TiO<sub>2</sub> підтверджує наявність дифракційних кілець на знімках електронної мікродифракції. Вміст в композиті титану по відношенню до кремнію менше ніж 1 % не дозволило виявити кристалічну фазу TiO<sub>2</sub> у композитах методом порошкової рентгенівської дифракції. Ймовірно, TiO<sub>2</sub> у композитах на основі високопористих SiO<sub>2</sub>-матриць присутній як у вигляді кристалітів, так і в аморфному стані.

Получены композиты SiO<sub>2</sub>:TiO<sub>2</sub> путем насыщения SiO<sub>2</sub>-матриц (с пористостью ~ 30 % и ~ 42 %) суспензией наночастиц TiO<sub>2</sub> и последующим отжигом до температуры 700°C. Показано, что в результате отжига композитов в интервале температур 400–700°C наблюдается агломерация наночастиц TiO<sub>2</sub> в порах SiO<sub>2</sub>-матрицы, что проявляется в увеличе-

нии поглощения в интервале длин волн 390–800 нм. Образование кристаллитов  $\text{TiO}_2$  в композитах  $\text{SiO}_2\text{:TiO}_2$  подтверждает наличие дифракционных колец на снимках электронной микродифракции. Содержание в композите титана по отношению к кремнию менее 1 % не позволяло обнаружить кристаллическую фазу  $\text{TiO}_2$  в композитах методом порошковой рентгеновской дифракции. Вероятно,  $\text{TiO}_2$  в композитах на основе высокопористых  $\text{SiO}_2$ -матриц присутствует как в виде кристаллитов, так и в аморфном состоянии.

## 1. Introduction

Organo-inorganic sol-gel hybrid compounds attract attention of researchers due to their ability to combine the functional properties of organic and inorganic constituents, uniformly distributed into a bulk of the samples, in one material. Today sol-gel synthesis is one of most diverse and promising methods of "soft" chemistry for creation of nanostructured oxides that can be effectively used in the field of photonics and photocatalysis [1]. An increased interest in nanoporous structures based on  $\text{SiO}_2$  synthesized by sol-gel method [2, 3] is due to the optical quality of these materials, and to a significant expansion of the field of their use for creation of new optoelectronic devices.  $\text{SiO}_2$ -matrices are highly transparent in Vis-NIR spectral range, and possess high mechanical and radiation resistance combined with high absorption capacity and chemical stability [2].

In a number of papers there is considered preparation of nanoporous silicate matrices with nanoparticles distributed in a macro-volume, including PbS nanocrystals with a diameter of 5–15 nm, for creation of narrow-band-gap semiconductors [4]. As shown in [5, 6], incorporation of metal oxide nanoparticles, in particular, titanium dioxide ( $\text{TiO}_2$ ) nanocrystals with a high cubic susceptibility ( $\chi^{(3)}$ ), into a dielectric matrix, increases the nonlinear optical (NLO) response of the matrix due to appearance of additional charge carriers. Such materials may find practical application in ultrafast optical switches and laser limiters [5, 6]. On the other hand, due to the presence of anion-exchange properties, for example, in highly porous silica-titanium matrices, they may effectively encapsulate dyes sensitive to pH, for creation of sensors to be used in determination of acidity of media. In particular, the obtaining of encapsulated indicator sol-gel silica-titania nanocomposite matrices was reported in [7]. In [8] there was considered creation and application of mesoporous  $\text{SiO}_2\text{-TiO}_2$  hybrid nanoparticles and thin films based on them as optical pH sensing and optochemical sensors. Nanoporous composites with high transparency in

the visible range of the spectrum can be used as photoactive media. For instance, in [9] amorphous  $\text{TiO}_2$  with long-range atomic disorder was shown to play an important role in photocatalytic performances and be used as a base for fabrication of novel amorphous nanomaterials for photochemical applications.

Nanostructured materials made from titanium dioxide ( $\text{TiO}_2$ ) are attractive for application in the fields of photocatalytic degradation of pollutants, photoreduction of carbon dioxide, and photocatalytic organic synthesis. As shown in [9], some physicochemical properties of  $\text{TiO}_2$ , such as light absorption, surface adsorption, separation of charge carriers, photocatalytic reactivity, etc. may be defined by disordered arrangement of its atoms. Amorphous materials have the typical structure of atomic disorder over long distances, and are isotropic both physically and chemically. Due to these properties they exhibit high activity in photocatalysis caused by efficient absorption of light and high specific surface area. The latter to a considerable extent defines the fact that amorphous  $\text{TiO}_2$  can play an important role in improvement of the photocatalytic activity of the material.  $\text{TiO}_2$  nanoparticles and clusters (synthesized from titanium tetra-iso-propoxide precursor) have an increased chemical activity [10, 11]. Moreover, they can be easily applied in the form of monolayer nanocoatings on substrates, as well as be incorporated into porous matrices.

The aim of this work was to synthesize  $\text{SiO}_2$ -matrices with variable density and porosity, to obtain  $\text{SiO}_2\text{:TiO}_2$  composites on their base by incorporating  $\text{TiO}_2$  nanoparticles into nanoporous  $\text{SiO}_2$ -matrices with subsequent annealing  $\text{SiO}_2\text{:TiO}_2$  to high temperatures, to study the structure as well as the spectral and luminescent properties of these composites.

## 2. Experimental

$\text{SiO}_2$ -matrices were synthesized using the sol-gel method by hydrolysis of tetraethoxysilane (TEOS; Aldrich) with the addition of nitric and hydrofluoric acids

(HF), ethanol and distilled water as described in [3, 12]. The solid xerogels were shaped as parallelepipeds with the dimensions  $\sim 0.45 \times 0.45 \times 1.5 \text{ cm}^3$ . The samples of pure  $\text{SiO}_2$ -matrices were annealed in air at temperatures up to  $700^\circ\text{C}$ , the rate of temperature rise was  $100^\circ\text{C/hr}$  and then  $150^\circ\text{C/hr}$ . The porosity of the matrices was estimated by the hydrostatic weighing method as in [12, 13].

Synthesis of amorphous titanium-oxo-alkoxo nanoparticles was carried out by the sol-gel method in a special reactor for preparation of nanostructured  $\text{TiO}_2$  with turbulent fast micromixing [10, 14]. Titanium (IV) isopropoxide/propan-2-ol (Alrich) and the mixture of  $\text{H}_2\text{O}$ /propan-2-ol were used as precursors, isopropanol being the solvent. The temperature of the reaction mixture was maintained to an accuracy of  $0.1^\circ\text{C}$ . As a result, there were obtained  $\text{TiO}_2$  clusters and  $\text{TiO}_2$  nanoparticles with a size of 2–5 nm which remained stable during the period from three hours to a day. The size of the nanoparticles was controlled using a fiber-optical probe by the method of dynamical scattering of He–Ne laser radiation.  $\text{SiO}_2:\text{TiO}_2$  composites were prepared by saturation of  $\text{SiO}_2$ -matrices (annealed to  $700^\circ\text{C}$ ) with  $\text{TiO}_2$  nanoparticles in isopropanol. Then the composites were dried at  $60^\circ\text{C}$  and annealed at temperatures up to  $400^\circ\text{C}$ ,  $550^\circ\text{C}$  and  $700^\circ\text{C}$  in air. After that  $\text{SiO}_2:\text{TiO}_2$  composites were annealed at  $700^\circ\text{C}$  during 4 hours. Two types of  $\text{SiO}_2$ -matrices were used for saturation by  $\text{TiO}_2$  nanoparticles: the ones with a porosity of  $\sim 30\%$  (type  $\text{SiO}_2$ -matrice (A)) and  $\sim 42\%$  (type  $\text{SiO}_2$ -matrice (B)). The porosity was regulated by the addition of HF acid in the synthesis of pure  $\text{SiO}_2$ -matrices. Accordingly, after saturation, there were obtained  $\text{SiO}_2:\text{TiO}_2(\text{A})$  and the  $\text{SiO}_2:\text{TiO}_2(\text{B})$  composites.

The absorption spectra of the samples were measured by means of a Lambda 35 UV/Vis Spectrophotometer (Perkin-Elmer, USA) in 200–1100 nm region. The luminescence spectra were obtained using a fluorimeter FluoroMax-4 (Horiba Jobin Yuon, USA). The infrared spectra of the crystals and of the powders were recorded using Spectrum One PerkinElmer at room temperature in  $400\text{--}4000 \text{ cm}^{-1}$  region with a resolution of  $1 \text{ cm}^{-1}$  by the KBr pellet technique. The structure of  $\text{SiO}_2$  xerogel was checked using a transmission electron microscope (TEM) (EM-125, SELMI, Ukraine) with an accelerating voltage of 100 kV. The samples for TEM investigation

were prepared by the following procedure: the samples of the composites were ground between two glass plates with subsequent deposition on a carbon film without preliminary sonication ( $\text{SiO}_2:\text{TiO}_2(\text{A})$ ) or after sonication during 30 sec in isopropyl alcohol ( $\text{SiO}_2:\text{TiO}_2(\text{B})$ ).

The crystalline structures of pure  $\text{SiO}_2$ -matrice,  $\text{SiO}_2:\text{TiO}_2$  composites annealed at temperatures up to  $580^\circ\text{C}$ ,  $\text{SiO}_2:\text{TiO}_2$  powder and quartz glass were investigated by a X-ray three-crystal diffractometer (TCD) in  $\text{CuK}_\alpha$ -radiation ( $\lambda = 1.54051 \text{ \AA}$ ) as in [15]. The phase composition of the synthesized  $\text{SiO}_2:\text{TiO}_2$  sample (annealed during 4 hours at  $700^\circ\text{C}$ ) was established by the method of X-ray phase analysis. For X-ray analysis there was used a Siemens D500 powder diffractometer ( $\text{CuK}_\alpha$  radiation, graphite monochromator, Bragg-Brentano geometry).

All the studies were performed at room temperature.

### 3. Results and discussions

There were synthesized pure  $\text{SiO}_2$ -matrices meant for their subsequent saturation with  $\text{TiO}_2$  nanoparticles for the making of  $\text{SiO}_2:\text{TiO}_2$  composites. It is known that HF acid used as a catalyst for the sol-gel process allows to synthesize  $\text{SiO}_2$ -matrices with a controlled porosity [3, 16]. Earlier, we obtained  $\text{SiO}_2$ -matrices with an open porosity from 32 % to 75 % [12] and used them for saturation with organic molecules [12, 13].

It should be noted that the structure of  $\text{SiO}_2$ -matrices saturation with a solution of nanoparticles is a branched system of  $\text{SiO}_2$  chains which form interconnected pores. At the same time, the samples of  $\text{SiO}_2$ -matrices should not be destroyed during their saturation with active additives. As shown in our paper [12], at the formation of the samples with a porosity less than 30 % and high density there arise additional stresses in the xerogel structure due to the appearance of a large number of small pores. Such  $\text{SiO}_2$ -matrices can be mechanically destroyed as a result of annealing, or upon saturation with the solutions, and introduction of the solution containing  $\text{TiO}_2$  nanoparticles into the bulk of such  $\text{SiO}_2$ -matrices may be difficult.  $\text{SiO}_2$ -matrices had pores with a size of 600 nm and more when their porosity increased above 55 % [12]. That may lead to the formation of cracks in the samples when they are saturated by the solution of  $\text{TiO}_2$  nanoparticles, as well as during drying and

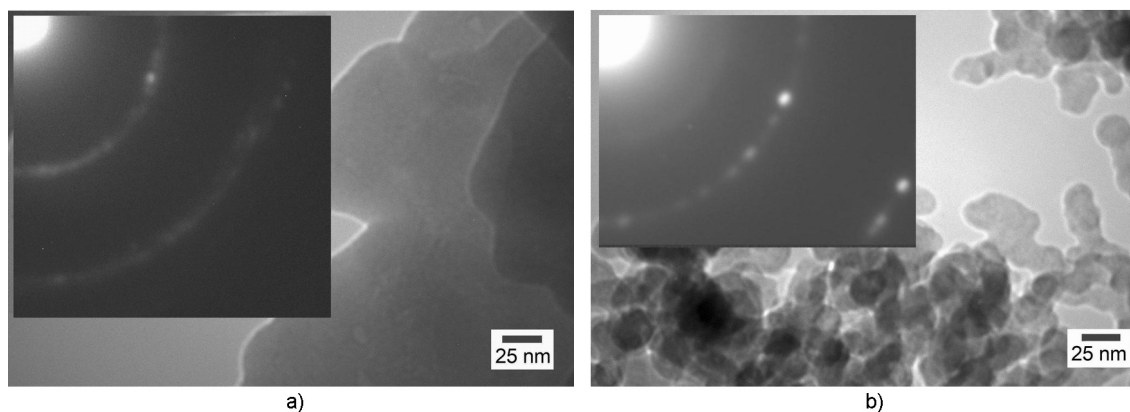


Fig. 1. TEM images of  $\text{SiO}_2\text{:TiO}_2$  (A) (a) and  $\text{SiO}_2\text{:TiO}_2$  (B) (b) composites annealed at a temperature up to  $580^\circ\text{C}$ .

annealing of the composites. Based on these factors, the matrices with an open porosity of 30–55 % were selected for the obtaining of  $\text{SiO}_2\text{:TiO}_2$  composite materials. The mass ratio of Ti:Si in the  $\text{SiO}_2\text{:TiO}_2$ (B) composite determined by atomic emission spectrometry was found to be  $8 \cdot 10^{-3}$  wt. %.

The morphology of  $\text{SiO}_2\text{:TiO}_2$  composites was investigated using TEM (Fig. 1a–c). We have previously shown [12] that the structure of pure  $\text{SiO}_2$ -matrices is formed by chains of 6–12 nm nanoparticles and small (5–12 nm) pores. There are also large pores with a size of 100–200 nm and more, which facilitate penetration of the solvent and  $\text{TiO}_2$  nanoparticles deep into the saturated  $\text{SiO}_2$ -matrices. As follows from Fig. 1a, the pores are not observed in the structure of  $\text{SiO}_2\text{:TiO}_2$ (A) composite. This is probably due to the filling of the pores with  $\text{TiO}_2$  nanoparticles. At the same time, the TEM image of the sample of  $\text{SiO}_2\text{:TiO}_2$ (B) subjected to ultrasonic treatment testifies to the presence of agglomerates with a size up to 29 nm which consist of smaller particles, and of the ones with a size up to 50 nm (Fig. 1b).

Using the methods of microdiffraction and X-ray structural analysis there were performed structural studies of the obtained composites (Fig. 1, Fig. 2). The presence of diffraction rings in the images of  $\text{SiO}_2\text{:TiO}_2$  (A) and  $\text{SiO}_2\text{:TiO}_2$ (B) composites measured using TEM points to possible formation of  $\text{TiO}_2$  crystallite phase (Fig. 1a,b). The curves of coherent scattering regions (CSR) of bulk samples of pure  $\text{SiO}_2$  matrices,  $\text{SiO}_2\text{:TiO}_2$ (B) composite, ground  $\text{SiO}_2\text{:TiO}_2$ (B) composite, and quartz glass are shown in the diffractograms (Fig. 2a) measured on a three-crystal diffractometer. All the curves are charac-

terized by the presence of a wide halo in the region of  $22\text{--}23^\circ$  with small CSR. This confirms amorphous structure of the studied samples, and is apparently due to amorphous structure of  $\text{SiO}_2$ -matrice itself [17]. An additional peak with larger CSRs for pure  $\text{SiO}_2$ -matrice (curve 1) and  $\text{SiO}_2\text{:TiO}_2$ (B) composite (curve 2) testifies to the presence of a bulk sample texture associated with peculiarities of xerogel formation. The surface texture was not analyzed due to the fact that the penetration depth of X-rays varied from hundredths to tenths of a millimeter, depending on the density of the material and radiation, thereat the size of the unit cell is usually much smaller (of the order of several angstroms or tens of angstroms).

According to the results of studying the samples of  $\text{SiO}_2\text{:TiO}_2$ (A) and  $\text{SiO}_2\text{:TiO}_2$ (B) composites (annealed at  $700^\circ\text{C}$  for 4 h) by powder diffraction, we can say that the phase  $\text{TiO}_2$  in the crystalline form is not observed in the samples (Fig. 2b). This is possibly due to the fact that the used method does not allow to reveal the presence of  $\text{TiO}_2$  nanocrystals at their low concentration in  $\text{SiO}_2$ -matrice (as mentioned above, Ti concentration with respect to Si does not exceed 1 %).

To estimate the effect of  $\text{TiO}_2$  nanoparticles on the surface state of the xerogel, there were measured IR spectra of  $\text{SiO}_2$ -matrices with different porosities before their saturation with  $\text{TiO}_2$  nanoparticles, and those of the finished samples (Fig. 3). The IR spectra of the samples have absorption bands with maxima at  $810\text{--}801\text{ cm}^{-1}$ ; a broad absorption band in the region of  $1080\text{--}1240\text{ cm}^{-1}$  with a maximum at  $1100\text{--}1080\text{ cm}^{-1}$ ; shoulder-shaped absorption

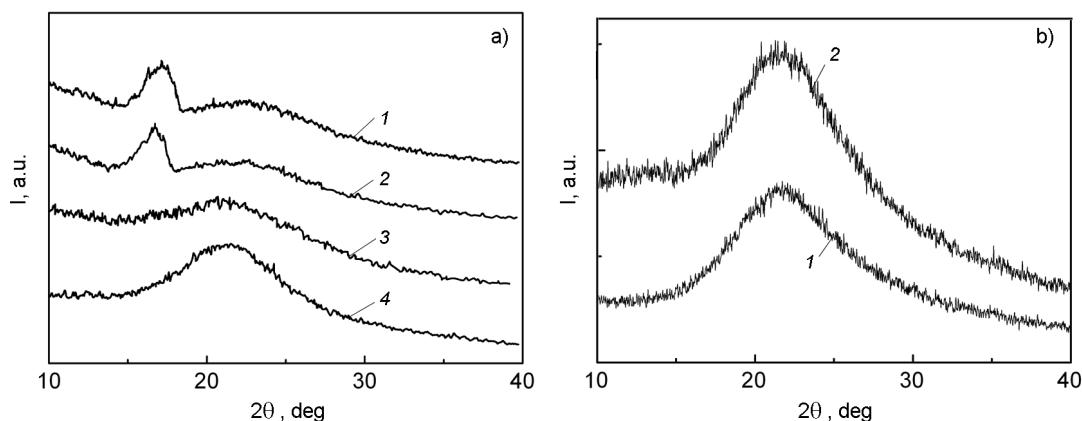


Fig. 2. Diffractograms of: pure  $\text{SiO}_2$  matrix (1),  $\text{SiO}_2:\text{TiO}_2$  (B) composite annealed at a temperature up to  $580^\circ\text{C}$  (2),  $\text{SiO}_2:\text{TiO}_2$ (B) powder from this composite (3), quartz glass (4) (a); and of  $\text{SiO}_2:\text{TiO}_2$  (A) (1) and  $\text{SiO}_2:\text{TiO}_2$ (B) (2) composites annealed during four hours at  $700^\circ\text{C}$  (b).

bands with maxima at  $1240\text{ cm}^{-1}$  and  $960\text{--}964\text{ cm}^{-1}$ ; and a band in the region of  $1750\text{--}1640\text{ cm}^{-1}$ . It should be noted that the bands with wavenumbers from  $1080\text{ cm}^{-1}$  to  $1200\text{ cm}^{-1}$  correspond to  $\text{Si-O(-Si)}$  vibrations, the band in the  $960\text{ cm}^{-1}$  region is bound up with  $\text{Si-O(H)}$  stretching vibrations, while the peak at  $\sim 1100\text{ cm}^{-1}$  is due to  $\text{Si-O(-Si)}$  stretching vibrations of a more linear structure of the xerogel [18]. The shift of the frequencies of stretching vibrations of  $\text{Si-O-Si}$  towards higher wavenumber values (higher frequencies) is correlated to strengthening of the network in the matrices [19]. The presence of the absorption peak in the region of  $1060\text{ cm}^{-1}$  for sol-gel  $\text{TiO-SiO}$  films, also observed in [20], may be attributed to asymmetric vibration of  $\text{Si-O-Si}$  bonds. In [21] the appearance of the peaks at  $793\text{ cm}^{-1}$  and  $1110\text{ cm}^{-1}$  was explained by symmetric and asymmetric  $\text{Si-O-Si}$  stretching vibration, respectively.

The position of the band bound up with  $\text{Si-O(-Si)}$  vibrations for pure  $\text{SiO}_2$ -matrices of type (A) and  $\text{SiO}_2:\text{TiO}_2$ (A) composite corresponds to the region of  $1083\text{ cm}^{-1}$  (Fig. 3, spectra 1 and 3). For pure  $\text{SiO}_2$ -matrices of type (B) and  $\text{SiO}_2:\text{TiO}_2$ (B) composite it is in the region of  $1096\text{ cm}^{-1}$  (Fig. 3, spectra 2 and 4) (Fig. 3, spectra 2 and 4). The initial  $\text{SiO}_2$ -matrices had different porosities:  $\sim 30\%$  for type (A) and  $\sim 42\%$  for type (B). For the synthesis of the former there was used a smaller amount of HF acid. The observed shift of the peak towards higher wavenumbers in the case of a higher HF concentration is in good agreement with our earlier investigation [12]. Note that in [12]

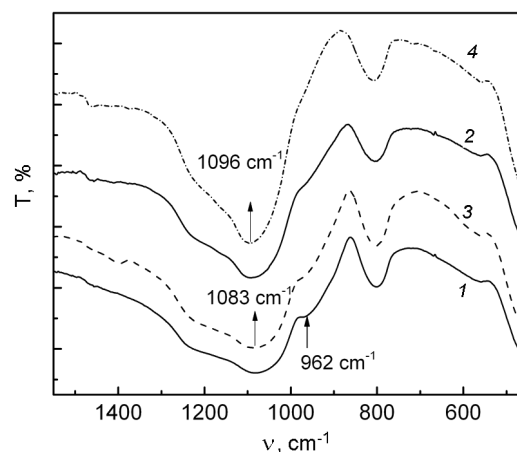


Fig. 3. FTIR-spectra of: pure  $\text{SiO}_2$ -matrix of type (A) (1), pure  $\text{SiO}_2$ -matrix of type (B) (2),  $\text{SiO}_2:\text{TiO}_2$ (A) composite (3),  $\text{SiO}_2:\text{TiO}_2$ (B) composite (4). Pure  $\text{SiO}_2$ -matrix and  $\text{SiO}_2:\text{TiO}_2$  composites were annealed at a temperature up to  $700^\circ\text{C}$ .

we reported a shift in the position of the peaks towards higher wavenumbers from  $1089\text{ cm}^{-1}$  to  $1104\text{ cm}^{-1}$  with an increase in HF concentration used in the synthesis of the matrices (when the porosity of matrices changed from 30 to 75 %).

Weakening of the absorption band intensity in the region of  $960\text{--}964\text{ cm}^{-1}$  (bound up with vibrations of  $\text{Si-O(H)}$  bonds [18]) in comparison with the intensity of the absorption bands of pure  $\text{SiO}_2$ -matrices of the type (A) (Fig. 3, spectra, 2) is clearly seen in the IR spectrum of  $\text{SiO}_2:\text{TiO}_2$ (A) composite (Fig. 3, spectra 3). At the same time, the absorption band in the region of  $960\text{--}964\text{ cm}^{-1}$  is not observed in the IR spectrum of  $\text{SiO}_2:\text{TiO}_2$ (B) composite (Fig. 3, spectrum 4). Such a

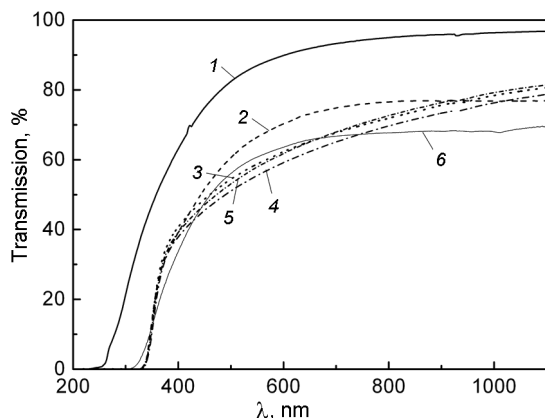


Fig. 4. Transmission spectra of pure  $\text{SiO}_2$ -matrix of type (B) without  $\text{TiO}_2$  (1),  $\text{SiO}_2:\text{TiO}_2$  (A) composite annealed at  $580^\circ\text{C}$  (6), and  $\text{SiO}_2:\text{TiO}_2$ (B) composite, annealed at temperatures of  $60^\circ\text{C}$  (2),  $400^\circ\text{C}$  (3),  $580^\circ\text{C}$  (4),  $700^\circ\text{C}$  (5). All pure  $\text{SiO}_2$ -matrices before saturation of  $\text{TiO}_2$  were previously annealed at a temperature up to  $700^\circ\text{C}$ .

change in the spectrum is probably due to the interaction of OH groups on the silica surface with  $\text{TiO}_2$  nanoparticles.

As seen from Fig. 4, pure  $\text{SiO}_2$ -matrix is highly transparent in the wavelength range of  $500\text{--}800\text{ nm}$ . Its spectral transmission is 90 % at  $600\text{ nm}$  and 95 % at  $800\text{ nm}$ . The transmission of pure  $\text{SiO}_2$ -matrices after its saturation with  $\text{TiO}_2$  nanoparticles decreases to 64 % and 68 % for  $\text{SiO}_2:\text{TiO}_2$ (A) composite (Fig. 4, spectrum 6) and to 70 % and 76 % for  $\text{SiO}_2:\text{TiO}_2$ (B) composite (Fig. 4, spectrum 2) for the wavelengths of  $600\text{ nm}$  and  $800\text{ nm}$ , respectively. Upon further an-

nealing of  $\text{SiO}_2:\text{TiO}_2$ (B) composite in the temperature range of  $400\text{--}700^\circ\text{C}$ , the transmission of the sample decreases to 62–58 % at  $600\text{ nm}$  and to 72–70 % at  $800\text{ nm}$  (Fig. 4, spectra 3–5).

The absorption spectra of pure  $\text{SiO}_2$ -matrices and  $\text{SiO}_2:\text{TiO}_2$ (B) composite annealed in the temperature range of  $400\text{--}700^\circ\text{C}$  are shown in Fig. 5a. The increase in the absorption value for the samples of  $\text{SiO}_2:\text{TiO}_2$ (B) composite in the wavelength range of  $410\text{--}800\text{ nm}$  is caused by consolidation of  $\text{TiO}_2$  nanoparticles in the pores of  $\text{SiO}_2$ -matrices due to possible formation of clusters from  $\text{TiO}_2$  nanoparticles at the annealing of the composite. This effect is especially noticeable in  $\text{SiO}_2:\text{TiO}_2$ (B) composite annealed at  $700^\circ\text{C}$  for 4 hours (Fig. 5, spectrum 6): in this case there is observed a significant increase in the absorption of the composite samples from  $\sim 370\text{ nm}$  towards larger wavelengths. According to [20],  $\text{TiO}$  nucleation in  $\text{TiO}_2\text{--SiO}_2$  films (synthesized from tetraethylorthosilicate and tetrabutyl titanate) occurs in the range  $550\text{--}750^\circ\text{C}$ .

As seen from the absorption spectra of  $\text{SiO}_2:\text{TiO}_2$ (B) composite (Fig. 5a), there is a shift of the edge of the fundamental absorption band in the composite relative to pure  $\text{SiO}_2$ -matrix by  $\sim 50\text{ nm}$  toward lower energies (i.e., to higher wavelengths). As is known, the position of the fundamental absorption edge of  $\text{SiO}_2:\text{TiO}_2$ (B) sample at  $3.6\text{ eV}$  corresponds to the band gap for amorphous oxo-alkoxy titanium nanoparticles [14]. Annealing of the composite at temperatures from  $400^\circ\text{C}$  to  $700^\circ\text{C}$  did not lead to a significant transformation of the absorption spectrum of the sample (Fig. 5a, b). Such a fact

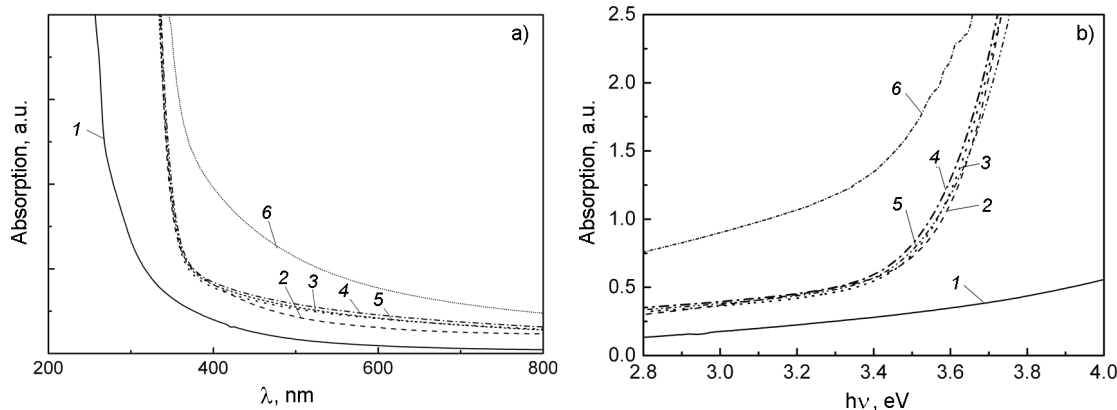


Fig. 5. Absorbance spectra of pure  $\text{SiO}_2$ -matrix of type (B) without  $\text{TiO}_2$  (1),  $\text{SiO}_2:\text{TiO}_2$ (B) composite annealed at temperature of  $60^\circ\text{C}$  (2), at temperatures up to  $400^\circ\text{C}$  (3),  $580^\circ\text{C}$  (4),  $700^\circ\text{C}$  (5) and annealed at  $700^\circ\text{C}$  during 4 hours (6) depending on wavelength (a) and energy (b). Before saturation with  $\text{TiO}_2$  all pure  $\text{SiO}_2$ -matrices were previously annealed at a temperature up to  $700^\circ\text{C}$ .

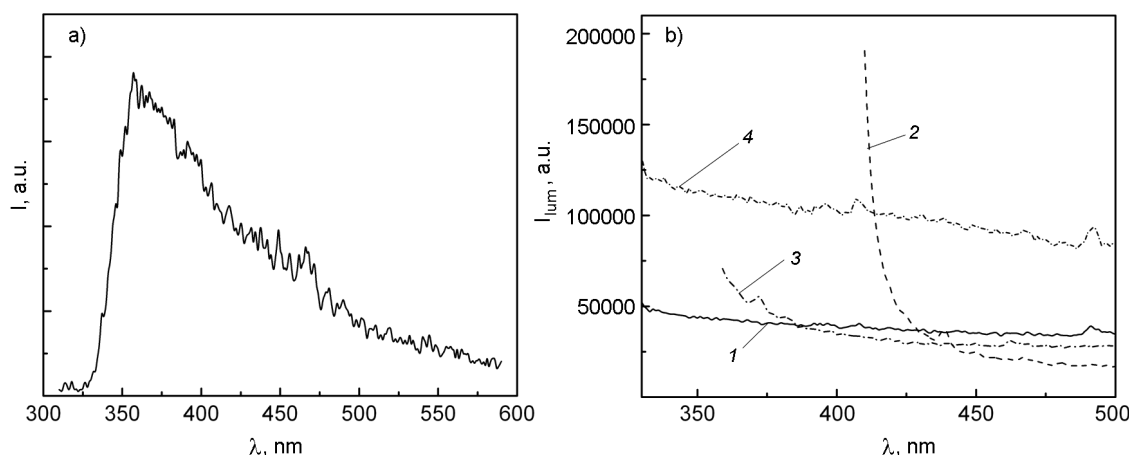


Fig. 6. Luminescence spectra of  $\text{SiO}_2:\text{TiO}_2$  (B) composite, annealed at a temperature up to  $700^\circ\text{C}$ ;  $\lambda_{ex} = 4.134$  eV (300 nm).  $\text{SiO}_2$ -matrix synthesized with HF and before saturation with  $\text{TiO}_2$  was previously annealed at a temperature up to  $700^\circ\text{C}$  (a); and luminescence spectra of pure  $\text{SiO}_2$ -matrices with a porosity of 23 % (1–3) and 55 % (4) (synthesized with HF and annealed at a temperature up to  $650^\circ\text{C}$ ).  $\text{SiO}_2$ -matrices were excited at:  $\lambda_{ex} = 300$  nm (1),  $\lambda_{ex} = 400$  nm (2),  $\lambda_{ex} = 340$  nm (3) and  $\lambda_{ex} = 300$  nm (4) (b).

may testify to the absence of formation of a significant amount of the crystalline phase of  $\text{TiO}_2$  [22].

Measurements of the photoluminescence spectra of pure  $\text{SiO}_2$ -matrix and of  $\text{SiO}_2:\text{TiO}_2$  composite showed that for the pure matrix luminescence was absent (as in [12]). In the luminescence spectrum of the composite there was observed a broad peak caused by radiative recombination of electron-hole pairs in  $\text{TiO}_2$  nanoparticles with a maximum at 362 nm (3.4 eV) [23] (Fig. 6a). This peak is most probably caused by electron transitions from deep traps inside the forbidden zone which are usually associated with disturbances of the structure of  $\text{TiO}_2$  nanoparticles caused by oxygen vacancies. Such defects are formed during preparation of  $\text{TiO}_2$  nanoparticles. A slight increase in the luminescence intensity in 2.7 eV (459 nm) region is probably bound up with luminescence of oxygen vacancies on the surface of  $\text{TiO}_2$  nanoparticles [23]. This peak is absent in the luminescence spectra of  $\text{TiO}_2$  nanoparticles with a minimum amount of oxygen vacancies, that, as a rule, agrees with the data in [24]. In addition, it is obvious that the high ratio of the surface-to-volume of  $\text{TiO}_2$  nanoparticle ensures the existence of a large number of oxygen vacancies on its surface. In the literature there are various data on the bands in the luminescence spectrum of  $\text{TiO}_2$  nanoparticles. For example, in [25] luminescence bands at 3.1, 3.19, 3.01 and 2.98 eV (at

$\lambda_{ex} = 330$  nm) were observed for crystalline  $\text{TiO}_2$  films annealed up to temperatures of  $200^\circ\text{C}$ ,  $300^\circ\text{C}$ ,  $400^\circ\text{C}$  and  $500^\circ\text{C}$ , respectively. Moreover, for amorphous  $\text{TiO}_2$  membranes there was observed a broad luminescence band with a maximum at 3.3 eV under excitation by X-ray radiation with an energy of 450 eV [26]. As shown in [20], nanostructured titanium dioxide also may have a luminescence band in the range of 360–550 nm.

It should be noted that the pure  $\text{SiO}_2$ -matrices synthesized in this work (annealed in the temperature range of  $500$ – $700^\circ\text{C}$ ) do not exhibit intrinsic luminescence upon excitation of luminescence in the wavelength range of 300–400 nm (Fig. 6b). This distinguishes our matrices from the sol-gel films containing  $\text{SiO}_2$ , which photoluminescence the authors of [20] attribute to oxygen related defects on Si leading to a blue emission band. So, luminescence in pure sol-gel  $\text{SiO}_2$  samples is probably influenced by the method of their preparation.

The annealing of the synthesized  $\text{SiO}_2:\text{TiO}_2$  composite to  $700^\circ\text{C}$  during preparation of the samples for measurement of the luminescence spectrum was caused by the fact that further increase in the annealing temperature could result in a worsening of the quality of  $\text{SiO}_2$ -matrix.

The presented  $\text{SiO}_2:\text{TiO}_2$  composites with  $\text{TiO}_2$  nanoparticles and nanocrystallites in an amorphous highly porous matrices may be used as photocatalysts.

At the same time, the pores that remain in the composites after saturation of SiO<sub>2</sub>-matrices with TiO<sub>2</sub> nanoparticles, may also cause light scattering. In the case of filling these pores with an optically transparent material, the scattering of light in the visible region of the spectrum can be reduced. Therefore, after filling these pores with polymethyl methacrylate (for example, polymerization of methyl methacrylate in the pores), light transmission by such a composite in the optical range can significantly rise. This makes it possible to use such a modified composite in photonics and may be a subject for further research.

#### 4. Conclusions

SiO<sub>2</sub>:TiO<sub>2</sub>(A) and SiO<sub>2</sub>:TiO<sub>2</sub>(B) composites were obtained by saturation of pure SiO<sub>2</sub>-matrices (with a porosity of ~ 30 % and ~ 42 %, respectively) with TiO<sub>2</sub> suspension and subsequent annealing at temperatures up to 700°C. Annealing of SiO<sub>2</sub>:TiO<sub>2</sub>(B) composite in the temperature range of 400–700°C increased the absorption in the visible spectral range, which might be caused by agglomeration of TiO<sub>2</sub> nanoparticles in the pores of SiO<sub>2</sub>-matrices. The observed luminescence of TiO<sub>2</sub> nanoparticles in SiO<sub>2</sub>:TiO<sub>2</sub>(B) composite in the range of 360–460 nm (at  $\lambda_{ex}$  = 300 nm) is due radiative recombination of charge carriers at deep defect levels formed by oxygen vacancies. The presence of diffraction rings in the electron microdiffraction images of the samples of SiO<sub>2</sub>:TiO<sub>2</sub>(A) and SiO<sub>2</sub>:TiO<sub>2</sub>(B) composites points to the presence of TiO<sub>2</sub> crystallites. However, the low (less than 1 %) concentration of titanium relative to silicon in the composite did not make it possible to reveal the presence of crystalline TiO<sub>2</sub> phase in the annealed composites by powder X-ray diffraction method. TiO<sub>2</sub> is present in SiO<sub>2</sub>:TiO<sub>2</sub>(A) and SiO<sub>2</sub>:TiO<sub>2</sub>(B) composites based on highly porous SiO<sub>2</sub>-matrices in the form of crystallites and in amorphous state, which allows to use them as photocatalysts.

*Acknowledgements.* This work was supported by a grant within the framework of the Ukrainian-French program DNIPRO. The authors are grateful to A.G.Yurkevych, Ph.D. V.F.Tkachenko, Ph.D. A.V.Lopin (Institute for Single Crystals) and Ph.D. A.Kanaev (Laboratoire des Sciences des Procédés et des Matériaux, French National Centre for Scientific Research, Paris, France) for their contribution to the present research.

#### References

1. C.Sanchez, L.Rozes, F.Ribot et al., *Comptes Rendus Chimie*, **13**, 3 (2010).
2. M.D.Rahn, T.A.King, *Appl. Opt.*, **34**, 8260 (1995).
3. R.Gvishi, U.Narang, G.Ruland et al., *Appl. Organ. Chem.*, **11**, 107 (1997).
4. L.Z.Yao, C.H.Ye, C.M.Mo et al., *J. Cryst. Growth*, **216**, 147 (2000).
5. I.M.Pritula, V.Ya.Gayvoronsky, M.I.Kolybaeva et al., *Opt. Mater.*, **33**, 623 (2011).
6. K.Uchida, S.Kanenko, S.Omi et al., *J. Opt. Soc. Am. B*, **11**, 1236 (1994).
7. S.Islam, N.Bidin, S.Riaz et al., *Sensors and Actuators B: Chemical*, **221**, 993 (2015).
8. S.Islam, N.Bidin, S.Riaz et al., *Sensors and Actuators B: Chemical*, **225**, 66 (2016).
9. S.Sun, P.Song, J.Cui et al., *Catal. Sci. Technol.*, **9**, 4198 (2019).
10. R.Azouani, A.Soloviev, M.Benmami et al., *J. Phys. Chem. C*, **111**, 16243 (2007).
11. P.Gorbovyi, A.Uklein, S.Tieng et al., *Nanoscience*, **3**, 1807 (2011).
12. O.N.Bezkrovnyaya, I.M.Pritula, A.G.Plakysyi et al., *J. of Non-Crystalline Solids*, **389**, 11 (2014).
13. O.N.Bezkrovnyaya, G.N.Babenko, I.M.Pritula et al., *J. Non-Crystalline Solids*, **535**, 119957 (2020).
14. A.Soloviev, R.Tufeu, C.Sanchez et al., *J. Phys. Chem. B*, **105**, 4175 (2001).
15. I.Pritula, O.Bezkrovnyaya, M.Kolybayeva et al., *Mater. Chem. Phys.*, **129**, 777 (2011).
16. E.Yariv, R.Reisfeld, Ts.Saraidarov et al., *J. Non-Crystalline Solids*, **305**, 354 (2002).
17. X.Zhang, H.Zheng, *Bull. Mater. Sci.*, **31**, 787 (2008).
18. N.Viart, D.Niznansky, J.L.Rehspringer, *J. Sol-Gel Sci. Tech.*, **8**, 183 (1997).
19. P.Innocenzi, G.Brusatin, M.Guglielmi et al., *Chem. Mater.*, **11**, 1672 (1999).
20. C.F.Song, M.K.Lu, P.Yang et al., *Thin Solid Films*, **413**, 155 (2002).
21. A.Amlouk, L.El Mir, S.Kraiem et al., *J. Physics and Chemistry of Solids*, **67**, 1464 (2006).
22. S.Valencia, J.M.Marin, G.Restrepo, *The Open Materials Science Journal*, **4**, 9 (2010).
23. J.Xu, L.Li, Y.Yan et al., *J. Colloid and Interface Sci.*, **318**, 29 (2008).
24. Y.Zhao, Ch.Li, X.Liu et al., *Mater. Lett.*, **61**, 79 (2007).
25. S.A.Abdullah, M.Z.Sahdan, N.Nafarizal et al., in: Intern. Seminar on Mathem. and Phys. in Sciences and Technol., 2017, Malaysia, J. Physics: Conf. Series, 995, 012067 (2018).
26. L.Liu, J.Li, T.-K.Sham, *Canadian J. Chemistry*, **93**, 1 (2015).